

Safety Risk Assessment of Shooting Test by Deep Learning Neural Networks



Chao Song, Yi-Zhuo Jia*, Dong-Jun Wang, Hong-Tian Liu, Yang Cao

Department of Weapons and Control, Army Academy of Armored Forces, Beijing, China
andysong2010@qq.com, tyututy@126.com, wdogw@sina.com, zgyluhongtian@sohu.com,
cy7979cy@163.com

Received 1 August 2020; Revised 1 September 2020; Accepted 23 September 2020

Abstract. To improve the safety of shooting tests in military tests, the safety risks of shooting tests are evaluated by the deep learning quantum gate circuit model, and the analysis of the vulnerability elements of the safety risk assessment is strengthened. The current safety management mechanism for shooting tests is analyzed. The practical experience of safety management is combined to build a quantum gate circuit neural network (QGCNN) model. The quantum revolving gate is utilized to control the qubit inversion and the phase deflection. The comprehensive risk value of shooting test safety is calculated. Simulation experiments have confirmed the reliability and effectiveness of the model, and the proposed model is compared with the traditional back propagation neural network (BPNN). The experimental results show that the proposed QGCNN has 28, 16, 14 and 12 iteration steps at different learning rates; for the output risk, the minimum error is 0.0025, and the maximum error is 0.0172, respectively; the performance of the proposed model is better than that of traditional BPNN. The constructed QGCNN model has a higher convergence rate for the safety risk assessment of shooting tests, which reduces the complexity of data processing, improves the accuracy of risk prediction.

Keywords: modeling, neural nets, risk analysis, safety management, shooting test

1 Introduction

With new military changes, many new-concept weapon projects have been established rapidly. In the meantime, the requirements for the research and development cycle, technology, and tactics continue to increase, while the safety risks in the research and development process have also increased. To ensure the safety of weapons, high-intensity prediction tests must be conducted in advance. However, there are many unstable factors during such tests, which may cause serious harms. Although many military research institutes have established safety management systems, the specific details still need to be improved. Through the identification of risk factors, evaluation and control, and the establishment of relevant normative systems, scientific and effective management and control will be performed to reduce the incidence of scientific research experiments, ensure the safety of personnel, and reduce the losses caused by scientific research [1-2]

Risk assessment plays a major role in industries that have critical requirements on safety. However, it also faces a series of challenges, such as technological progress and increasing demand. At present, scholars have focused on continuous risk assessments, improving previous learning models, and defining techniques for processing the data. At the same time, it is necessary to have sufficient capacity to handle emergencies and provide correct support for risk management. Deep learning-related models have reasonable accuracy in assessing safety risks, which can overcome the challenges of risk assessment. However, the limitations of the inherent model should be considered, and appropriate model selection and customization should be carefully performed to provide appropriate support for safety-related decisions [3].

* Corresponding Author

The safety management system was introduced in the 1980s to reduce the risks of injury and death, and minimize material waste in the construction industry. Yiu et al. (2019) reviewed previous researches to determine the benefits and obstacles of implementing a safety management system and conducted a questionnaire survey to determine the major benefits and obstacles of implementing short message services (SMS) in the construction industry, thereby contributing to the current knowledge system of safety research [4]. Lee et al. (2016) explored the systematic changes in laws, regulations, corporate culture, accident response, and other aspects of chemical safety management at the national level after major chemical spill accidents, and formulated more practical plans and guidance policies [5]. In recent years, deep learning has been widely utilized in various types of risk assessments in different fields, such as financial risk management, disease risk assessment, aviation safety risk assessment, and crude oil market assessment [6-7]. The powerful data processing capabilities of deep learning are widely concerned by scholars in China. Due to the various uncertainties in the process of shooting tests, researchers are trying to formulate more accurate and comprehensive criteria for extracting risk factors. However, it still requires in-depth study to test the criteria for risk factors that improve the performance of the risk assessment model.

The above description shows that despite the various researches on site safety, explorations of military shooting test grounds are rare. Here, the original data of the XXX Weapon Institute are utilized for training, and the quantum gate circuit model is applied to evaluate the shooting risks and the performance of the proposed model, which provides a reference for the safety risk assessment and management of the shooting tests.

2 Method

2.1 Classification of Risk Factors

According to the *Classification and Code of Dangerous and Hazardous Factors in the Production Process* (GB/13861-2009) issued by the central government of China, the harmful factors are divided into the following four aspects:

(1) Human factors

Psychological and physiological harmful factors: overload limit, such as hearing load limit, visual load limit, and physical load limit; engaging in taboo operations; abnormal health conditions; emotional abnormalities, such as psychological abnormalities; defects in identifying function, such as recognition errors; perception delays.

Behavioral harmful factors: command errors, such as illegal command and command faults; operation errors, such as illegal operations, misuse, and custody errors.

(2) Factors of things

Chemical harmful factors: flammable liquids; explosives; flammable solids, natural objects and flammable materials in contact with moisture; corrosives; dangerous compressed gases and liquefied gases; toxic drugs; oxidants and organic peroxides.

Physical harmful factors: defects in facilities, equipment, accessories, and tools, such as insufficient rigidity, insufficient strength, poor stability, poor corrosion resistance, poor sealing, defective appearance, stress concentration, and brake or controller defects; protection defects: no protection, improper protection, insufficient protection distance, improper support, protective device, and facility defects; electrical injury: leakage, static electricity, lightning, and sparks; noise: electromagnetic noise, mechanical noise, and hydrodynamic noise; vibration hazards: electromagnetic vibration, mechanical vibration, and hydrodynamic vibration; ionizing radiation: X-rays, γ rays, α particles, β particles, neutrons, protons, and high energy electron beams; non-ionizing radiation: ultraviolet radiation, microwave radiation, laser radiation, ultra-high frequency radiation, power frequency electric field, and high frequency radiation; sports injuries: splashes, projectiles, rebounds, falling objects, soil, rock sliding, and airflow scrolling; open flames; high temperature objects: high temperature liquids, gases, and solids; low temperature objects: low temperature liquids, gases, and solids. Signal defects: no signal, improper signal selection or improper position, inaccurate signal display, and unclear signal; sign defects: no sign, unclear sign, irregular, defective position, and improper selection. Harmful lights: glare and stroboscopic effect.

Biological harmful factors: pathogenic microorganisms, such as bacteria, fungi, and viruses; vectors of

infectious diseases; harmful plants; harmful animals, and other harmful factors.

(3) Environmental factors: indoor, outdoor, above ground, underground (such as tunnels and mines), water, underwater, and other operating construction environments.

(4) Management factors: the occupational safety and health responsibility systems have not been implemented, and the organizational structure is not perfect; the “three-simultaneous system” for construction projects has not been implemented; the occupational safety and health management regulations are not perfect, and the operation procedures are not standardized; the training system is not perfect; there are no emergency plans and responses; imperfect occupational health management; insufficient occupational safety and health investment.

2.2 Safety Risk Assessment Methods of Shooting Test

(1) Preliminary hazard analysis

Preliminary hazard analysis (PHA) refers to the macro and rough analysis of various risk factors (category and distribution) and occurrence conditions before an engineering activity, such as design, construction, production, and maintenance, as well as systematic safety analytical methods for the possible consequences of accidents. Its major function is to identify the cause of the hazard, recognize the main hazards associated with the system, assess the consequences of the accident, and propose protective measures to control or eliminate the hazard [8-9].

(2) Risk assessment method for operating conditions

The Likelihood-Exposure-Criticality (LEC), a risk assessment method for working conditions, is a simple and convenient semi-quantitative evaluation method for the risk of employees working in potentially hazardous environments. Proposed by K.J. Graham and G.F. Kinney, this method includes the following influencing factors: the likelihood (L) of an accident, the frequency of human exposure (E) to this dangerous environment, and the criticality (C) of damage in the event of this accident. Based on the on-site operating conditions, experts familiar with the operating conditions will score L, E, and C according to the prescribed standards. The average of the three component values are taken as the calculated scores of L, E, and C, and the calculated danger (D) score is utilized to evaluate the hazard level of the operating conditions. The equation for dangers of operating condition is:

$$D = L * E * C \quad (1)$$

However, since this method defines the degree of risks and determines the scores of the three factors based on expert experiences, it has limitations, and the evaluation should be adjusted appropriately according to the specific situations.

2.3 LEC Method Combined with Fuzzy Evaluation Method

Here, the LEC method is combined with fuzzy evaluation method to evaluate the risks in shooting tests and propose the control measures [10-13]. Experts in the fields of scientific research projects, professional technical management, and safety management are chosen to effectively reflect the dangers through scoring. The risk factors of operating conditions are shown in Table 1. The risks of operating conditions are obtained by Equation (1) and corresponds to the corresponding risk indicator R, as shown in Table 2.

Table 1. Value criteria for influencing factors of risk assessment methods for operating conditions

Likelihood(L)	Score	Exposure(E)	Score	Criticality(C)	Score
Completely expected	10	Continuous	10	More than ten people died	100
Quite possible	6	Every day	6	Several people died	40
Infrequent but possible	3	Once a week	3	One dead	15
Very unlikely	1	Once a month	2	Severely disabled	7
Conceivable but rarely possible	0.5	Once a year	1	Disabled	3
Highly unlikely	0.2	Rare	0.5	Minor injuries	1
Practically impossible	0.1				

Table 2. Criteria for the classification of danger degrees

Risk score	Risk factor	Degrees	Classification
≥ 320	$0.6 \leq R < 1$	Extremely dangerous	Level 1
$\geq 160 \sim 320$	$0.6 \leq R < 0.8$	Highly dangerous	Level 2
$\geq 70 \sim 160$	$0.4 \leq R < 0.6$	Significantly dangerous	Level 3
Risk score	Risk factor	Degrees	Classification
≥ 320	$0.6 \leq R < 1$	Extremely dangerous	Level 1

By analyzing the risk factors of the five positions during the shooting tests and their possibility, the risks of the shooting tests are analyzed, and the risk factors of these positions with greater risks and may have more serious consequences are extracted, managed, and controlled. According to the LEC method in combination with the fuzzy evaluation method, the degree of danger of each position is analyzed quantitatively, as shown in Table 3.

Table 3. Average evaluation scores by LEC experts in five positions

Shooting experiment post	Likelihood(L)	Exposure(E)	Criticality(C)	Degrees
Artillery test	4	4	16	256
Shooting range test	0.8	4	12	38.4
Ammunition management	4	5	17	272
Mechanical maintenance	0.5	3	1	1.5
Late guarantee	0.4	2	1.5	1.2

The results show that the ammunition management and artillery test positions have a risk degree score greater than 160 points, which is at high risk; meanwhile, the risk score of the whip field test position is 38.4 points, which is at potential risk and requires observation. The scores of the two positions of logistics support and mechanical maintenance are below 2 points, which is not dangerous. Therefore, it is necessary to focus on strengthening the safety management of the two positions of new artillery shooting and ammunition management.

2.4 Risk Assessment Indicator Model

The risk assessment indicator system model is shown in Fig. 1. The first-level indicator $M_i (i = 1, 2, \dots, m)$ is dominated by the top-level target M, the second-level indicator $M_{ij} (i = 1, 2, \dots, m, j = 1, 2, \dots, n)$ is dominated by the first-level indicator, and the rest may be deduced by analogy to form a top-down hierarchy model. The indicators are independent of each other, with obvious crossovers, avoidance of inclusion, and implicit relationships, thereby ensuring the independence of the assessment indicators and reflecting the assessment content of some aspect of the system. It includes first-level indicators a, b , and second-level indicators ab, ac . The selected indicators should satisfy the following relationship:

$$ifa \neq b \Rightarrow M_a \cap M_b = \emptyset (a, b = 1, 2, \dots, m) \tag{2}$$

$$\forall ab \neq ac \Rightarrow M_{ab} \cap M_{ac} = \emptyset \begin{pmatrix} a = 1, 2, \dots, m \\ b, c = 1, 2, \dots, n \end{pmatrix} \tag{3}$$

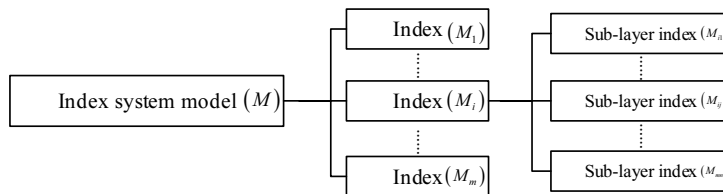


Fig. 1. The indicator system model of risk assessment (M)

The risk assessment and inspection should be based on GB/T13861-2009 *Classification and Code of Dangerous and Hazardous Factors in Production Process* and GB 0441-86 *Classification Standards of Enterprise Casualty Accidents*. The risk management should be in accordance with the recommended standard GB/T 27921-2011 *Risk Management and Risk Assessment Technology*. The indicator system for shooting test safety risk assessment is constructed, as shown in Fig. 2. In the constructed shooting test hierarchical model, from top to bottom are the target layer, the criterion layer, and the factor layer.

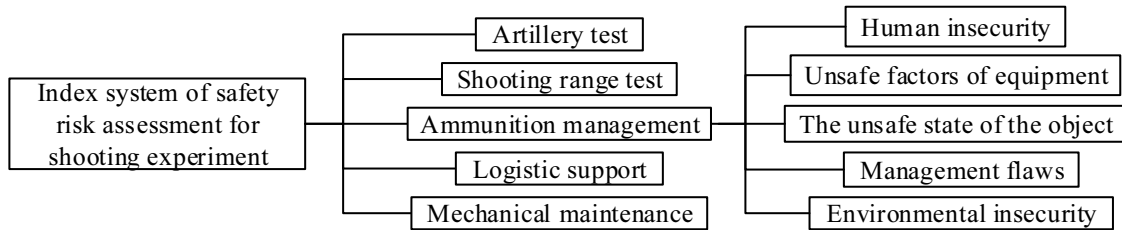


Fig. 2. Shooting test safety risk assessment indicator system

The ammunition management position is taken as an example, the safety risk factors related to ammunition management are developed and analyzed according to the standards and requirements of GB/T13861-2009 *Classification and Code of Hazardous and Factors in the Production Process*.

2.5 Data Preprocessing

According to the risk evaluation indicator model constructed above, the safety inspection and test of the shooting test are conducted to obtain the evaluation dataset. The data are divided into qualitative indicators and quantitative indicators, and the corresponding pre-processing of the indicator data is convenient for the calculation of risk assessment. For qualitative indicators, data preprocessing is to complete the quantification of indicators and eliminate the difference in description of indicators; for quantitative indicators, data preprocessing is to reduce the dimension and eliminate dimensional differences between indicators.

(1) Standard quantification method

Through this method, the qualitative indicator data are quantified. The qualitative indicators are divided into n grades, which are denoted as a_1, a_2, \dots, a_n , and the five-level scoring is used for classification, as shown in Table 4. The qualitative indicators can be divided into positive and negative indicators. The positive indicator is that when the attribute value is larger, the performance is better.

Table 4. Gradation indicator gradient

Classification	Failed	Qualified	General	Good	Excellent
Positive indicator	1	2	3	4	5
Reverse indicator	5	4	3	2	1

(2) Feature vector quantization method

If there are n indicator data A_1, A_2, \dots, A_n , the corresponding weight is $\omega_1, \omega_2, \dots, \omega_n$, the ratio of any two weights is determined, and the indicator data weight ratio matrix A is calculated, as shown in Equation (4):

$$A = \begin{bmatrix} \frac{\omega_2}{\omega_1} & \frac{\omega_2}{\omega_2} & \dots & \frac{\omega_2}{\omega_n} \\ \vdots & \vdots & & \vdots \\ \frac{\omega_n}{\omega_1} & \frac{\omega_n}{\omega_2} & \dots & \frac{\omega_n}{\omega_n} \end{bmatrix} = (a_{ij})_{nn} \tag{4}$$

When A satisfies $a_{ij} = 1/a_{ji}$ and $a_{ii} = 1 (i, j, k = 1, 2, \dots, n)$, it is multiplied by the weight vector

$W = [\omega_1, \omega_2, \dots, \omega_n]^T$ to derive:

$$AW = nW \tag{5}$$

The weight matrix W is the largest eigenvector and feature root of the matrix A . The result of weight ranking is obtained by the above equation, and the order quantification of qualitative indicator data is realized.

(3) Quantitative indicator processing: range transformation method

If there is an indicator data x_1, x_2, \dots, x_n , its range is transformed:

$$y_i = \frac{x_i - \min\{x_i\}}{\max\{x_i\} - \min\{x_i\}} \quad (i = 1, 2, \dots, n) \tag{6}$$

Where $y_i \in [0, 1]$. For quantitative indicator data, 1 indicates the best attribute value, and 0 indicates the worst attribute value.

2.6 Theoretical Basis of Quantum Gate Circuit Neural Network (QGCNN)

Quantum information technology can process data volume problems with uncertainty and large data volume, which improves the accuracy of data processing and the execution efficiency of algorithms [14-17]. Research by Shao (2020) et al. proved that the universality of multi-bit controlled NOT (CNOT) gate and one-bit phase shift gate can be used to complete any two-level unitary operation of n qubit state space; any quantum gate circuit can be decomposed into the product form of a phase shift gate and multi-bit CNOT gate [18]. Therefore, the versatility of the two are utilized to construct a QGCNN model through the quantum gate circuit; then, the model is applied to the safety risk assessment of the shooting test to optimize the evaluation calculation. The quantum gate circuit is shown in Fig. 3.

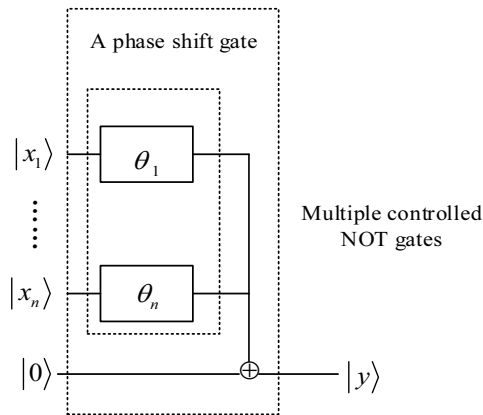


Fig. 3. Quantum gate circuit

The initial quantum state is $|\varphi\rangle = \begin{bmatrix} \cos\theta_0 \\ \sin\theta_0 \end{bmatrix}$, X represents a single-bit CNOT gate, R represents a one-bit phase shift gate, $|x_1\rangle, |x_2\rangle, \dots, |x_n\rangle$ represents a quantum state input signal, $\theta_i (i = 1, 2, \dots, n)$ represents a phase shift angle; if n controlling qubits are $|x_i\rangle = \alpha_i|0\rangle + \beta_i|1\rangle (i = 1, 2, \dots, n)$, the output of the quantum gate circuit structure model $|y\rangle$ is expressed as follows:

$$|y\rangle = C^n(X)(R(|x_i\rangle)) \otimes |0\rangle \tag{7}$$

Through the above-mentioned quantum gate circuit, a model of QGCNN is established, as shown in Fig. 4. The QGCNN model is divided into three layers, i.e., the network input layer, the hidden layer, and the output layer.

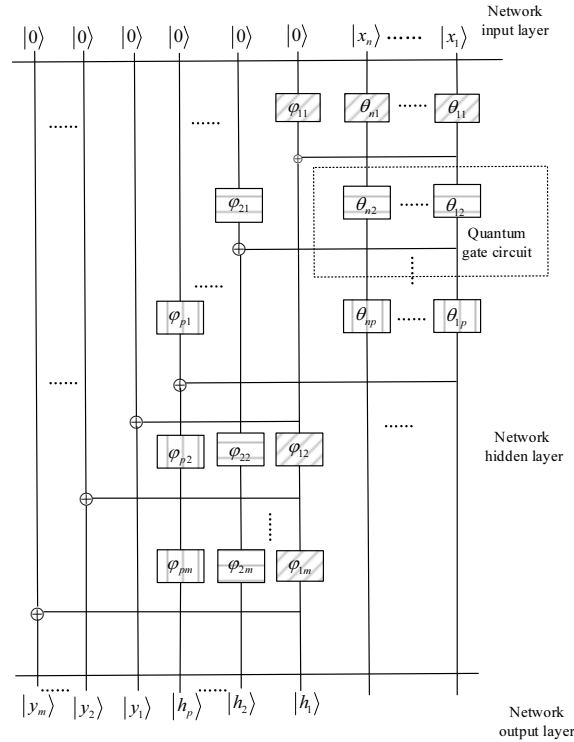


Fig. 4. QGCNN model

Where $|x_1\rangle, |x_2\rangle, \dots, |x_n\rangle, |x_i\rangle (i=1, 2, \dots, n)$ represents the input layer qubit, which is rotated by the phase shift gate to control the inversion of the hidden layer qubit; $|h_1\rangle, |h_2\rangle, \dots, |h_p\rangle, |h_j\rangle (j=1, 2, \dots, p)$ represents the output of the hidden layer, which is rotated by the phase shift gate to control the inversion of the qubits of the output layer; $|y_1\rangle, |y_2\rangle, \dots, |y_m\rangle$ represents the output of the output layer. The deep learning algorithm and output of each layer are described as follows: the input qubit is represented as $|x_i\rangle = \cos\theta_i|0\rangle + \sin\theta_i|1\rangle (i=1, 2, \dots, n)$, and each layer takes the probability amplitude of the qubit state $|1\rangle$ as the actual output of the layer. The actual output h_j and y_k of the hidden layer and the output layer are expressed as:

$$h_j = \sin(\psi_j) = \prod_{i=1}^n \sin(\theta_i + \theta_{ij}) \tag{8}$$

$$y_k = \prod_{j=1}^p \sin\left(\arcsin\left(\prod_{i=1}^n \sin(\theta_i + \theta_{ij})\right) + \psi_{jk}\right) \tag{9}$$

Where $i=1, 2, \dots, n, j=1, 2, \dots, p, k=1, 2, \dots, m, \theta_{ij}$ and ψ_{jk} are the adjustable parameters of the model, which respectively represents the rotation angle of the phase shift gate of the hidden layer and the output layer. If $\tilde{y}_1, \tilde{y}_2, \dots, \tilde{y}_m$ is used as the expected output value of the model, the error function E can be expressed as:

$$E = \frac{1}{2} \sum_{k=1}^m (\tilde{y}_k - y_k)^2 \tag{10}$$

The gradient descent method calculates that the partial derivative of error E with respect to rotation angles θ_{ij} and ψ_{jk} :

$$-\frac{\partial E}{\partial \theta_{ij}} = \frac{\sum_{k=1}^m (\tilde{y}_k - y_k) y_k \cot(\psi_j + \psi_{jk}) h_j \cot(\theta_i + \theta_{ij})}{\sqrt{1 - h_j^2}} \quad (11)$$

$$-\frac{\partial E}{\partial \psi_{j1}} = \sum_{k=1}^m (\tilde{y}_k - y_k) y_k \cot(\psi_j + \psi_{jk}) \quad (12)$$

The above equations are updated:

$$\theta_{ij}(t+1) = \theta_{ij}(t) - \eta \frac{\partial E}{\partial \theta_{ij}} \quad (13)$$

$$\psi_{jk}(t+1) = \psi_{jk}(t) - \eta \frac{\partial E}{\partial \psi_{jk}} \quad (14)$$

Where t represents the iteration number of the network, η represents the learning rate of the network. y_k represents the actual output value, \tilde{y}_k represents the expected output value, and the relationship between the two is expressed as:

$$y_k = \prod_{j=1}^p \sin \left(\arcsin \left(\prod_{i=1}^n \sin(\theta_i + \tilde{\theta}_{ij}) \right) + \tilde{\psi}_{jk} \right) \quad (15)$$

If $\tilde{\theta}_{ij}$ and $\tilde{\psi}_{jk}$ are respectively expressed as global optimal solutions of iteration sequences $\{\theta_{ij}(t)\}$ and $\{\psi_{jk}(t)\}$, for any integers n_1 and n_2 , rotation angles $\bar{\theta}_{ij} = 2n_1\pi + \tilde{\theta}_{ij}$ and $\bar{\psi}_{jk} = 2n_2\pi + \tilde{\psi}_{jk}$ are also global optimal solutions of iteration sequences $\{\theta_{ij}(t)\}$ and $\{\psi_{jk}(t)\}$. Similarly, y_k and \tilde{y}_k satisfy the following relationship:

$$y_k = \prod_{j=1}^p \sin \left(\arcsin \left(\prod_{i=1}^n \sin(\theta_i + \tilde{\theta}_{ij}) \right) + \tilde{\psi}_{jk} \right) = \tilde{y}_k \quad (16)$$

According to Equations (15) and (16), iterative sequence $\{\theta_{ij}(t)\}$ and $\{\psi_{jk}(t)\}$ have periodic global optimal solutions in $[\alpha, \alpha + 2\pi]$, and α is any integer. Therefore, this model has many global attractors and the number of optimal solutions, which improves the convergence speed and accuracy of the network.

2.7 Network Training Process

To reduce the complexity of the system, the risk assessment model is split; after the data sample is preprocessed, the quantum state description is used as the network input vector. After the neural network model is trained and tested, the combined neural network is obtained, and the overall risk assessment of the shooting test is conducted. The shooting test is split into d subsystems $S_i (i=1, 2, \dots, d)$, as shown in Fig. 5. The input layer in the subsystem is the attribute value $x_{ij} (i=1, 2, \dots, d, j=1, 2, \dots, n)$ of each safety risk factor in the shooting test; $\omega_{io} (i=1, 2, \dots, d, o=1, 2, \dots, m)$ represents the hidden layer connection weight; the final output layer is a single node output, and the calculated risk value $y_{il} (i=1, 2, \dots, d, l=1, 2, \dots, k)$ is output; finally, the overall safety risk value Y of the shooting test is calculated. The target layer, criterion layer, and factor layer of the risk assessment indicator model correspond to the output layer, hidden layer, and input layer in the combined neural network, respectively.

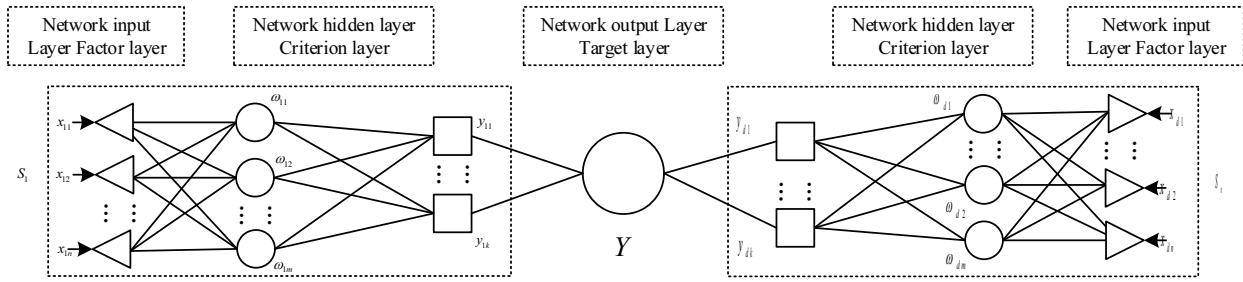


Fig. 5. Neural network combination model

The values of the number of neurons in the hidden layer of the network are as follows:

$$l = \log_2 n \tag{17}$$

Where n represents the number of nodes in the input layer of the network, and l represents the number of nodes in the hidden layer of the network. After the training is completed, the data sample $X^i (i = 1, 2, \dots, m)$ to be evaluated is selected randomly; then, it is input into the network after the training, and its risk value is output. The error calculation is performed on the actual and expected output values of the evaluation samples, i.e., error calculation of y_i and \tilde{y}_i , $e_i = |y_i - \tilde{y}_i|$. The risk assessment and analysis of shooting test safety is completed by calculating the relative and absolute errors of the network.

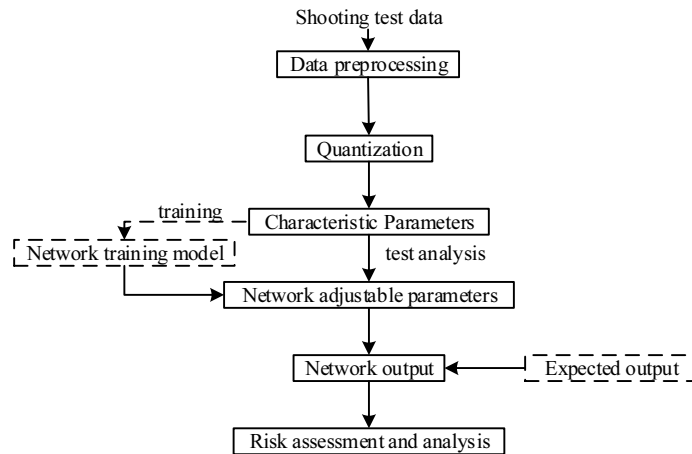


Fig. 6. QGCNN shooting test safety risk assessment process

2.8 Simulations Experiments

The environment of this simulation experiment is a device with Central Processing Unit (CPU) model Pentium G640, Matlab2014b, Windows 7 operating system, and 8GB memory. The performance of the proposed QGCNN is compared with that of the traditional BPNN. The information safety risk assessment of the QGCNN managed by the subsystem ammunition is taken as an example, the effectiveness and reliability of the verification method are verified. Ammunition management safety (2S) contains seven risk factors, which are carrying tinder or mobile phone (1x), snorkel stacking that does not meet the specifications or excess (2x), combustible materials in the protection dike (3x), personnel without a certificate or untrained personnel (4x), imperfect management system (5x), damage to fire-fighting equipment and facilities (6x), unpacking and processing of ammunition do not follow the requirements (7x). The data obtained from the safety inspection of the shooting test of the XXX Weapon Institute is used as the training set and test set of the experiment. The sample data is preprocessed to obtain the evaluation sample data. Among them, 10 groups are selected as the training set and 5 groups are the test set. The expected output is given comprehensively based on the national recommended standards GB/T13861-2009 *Classification and Code of Dangerous and Hazardous Factors in Production Process* and GB-T6441-1986_1 *Classification Standards of Enterprise Casualty Accidents*.

A three-layer QGCNN model of subsystem ammunition management safety (2S) is built. The input

layer contains 7 neuron nodes to receive the risk factor x_i ($i = 1, 2, \dots, 7$). According to Equation (17), the number of neurons in the hidden layer is $i = \log_2 7 \approx 3$. Therefore, the neural network has a 7-3-1 three-layer structure with a maximum iteration step number of 1000 and a training error accuracy of 0.0001. Finally, a comparative experiment with the traditional BPNN is performed. The learning rate of the network is selected as 0.3, 0.5, 0.8, and 1.0. When the training error is less than the set error accuracy, or the iteration step reaches the set maximum iteration step, the training is completed, and the simulation experiment results are analyzed.

3 Results and Discussion

3.1 Comparison of Iteration Steps of Two Neural Networks in Different Learning Efficiencies

The performance curves of the two neural networks being trained at a learning rate of 1.0 are shown in Fig. 7. The experimental results show that both can effectively converge. Besides, the number of iteration steps with different learning rates is shown in Table 5. Here, the iterative steps of different learning rates of the proposed QGCNN are 28, 16, 14 and 12; for traditional BPNN, the iterative steps of different learning rates are 52, 27, 23 and 18. Therefore, the proposed QGCNN model has a faster convergence speed.

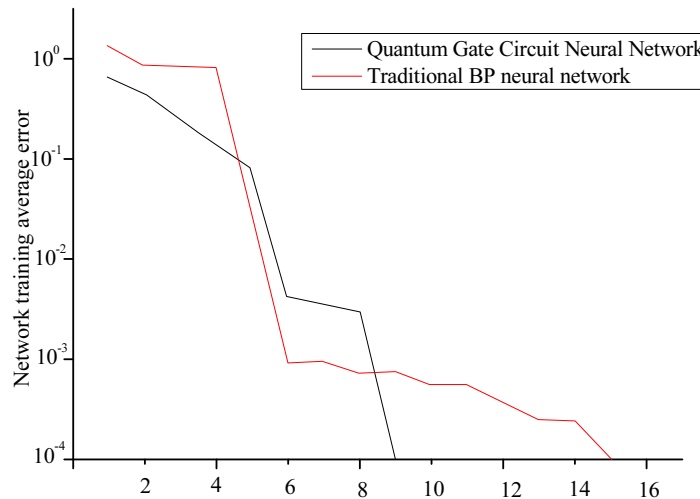


Fig. 7. Network training performance curves with a learning rate of 1.0

Table 5. Iterative steps of networks with different learning rates

Learning rate	0.3	0.5	0.8	1.0
Traditional BPNN	52	27	23	18
QGCNN	28	16	14	12

Table 5 shows that under different learning rates, the designed algorithm has less iterative steps than BPNN, showing the advantages in training time.

3.2 Results of Sample Risk Assessment by the Two Neural Networks

Both neural networks can effectively assess the risk value of the samples, and the prediction results are shown in Fig. 8. The minimum error between the proposed QGCNN model and the traditional BPNN is 0.0025 and 0.0065, and the maximum error is 0.0172 and 0.0492, respectively. The results show that the error of the constructed QGCNN is smaller, and its risk prediction ability is better. The calculation results are shown in Table 6.

Table 6. The risk errors output by two kinds of neural networks

Test sample	QGCNN		Traditional BPNN		Expected output
	Actual output	Test error	Actual output	Test error	
1	0.5210	0.0034	0.5024	0.0103	0.52
2	0.4932	0.0157	0.4758	0.0065	0.48
3	0.5096	0.0025	0.5406	0.0492	0.51
4	0.5153	0.0172	0.5107	0.0124	0.50
5	0.5184	0.0109	0.5012	0.0285	0.52
Average error	0.0112		0.0187		
Standard deviation	0.0054		0.0115		

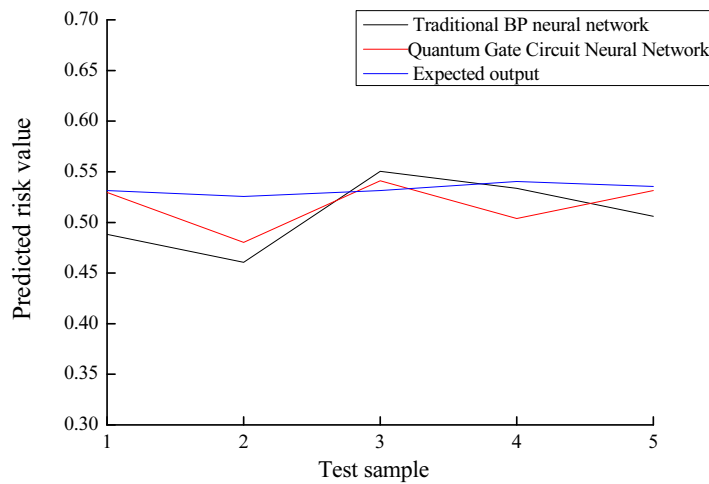


Fig. 8. Two neural network risk assessment test results

The average relative errors of the two neural network risk predictions are 2.39% and 3.71%, respectively, and the calculation results are shown in Table 7. The results show that the risk prediction accuracy of the constructed QGCNN is better.

Table 7. Relative error of risk prediction (%)

Algorithm	1	2	3	4	5	Average error
QGCNN	1.65	3.72	0.54	3.05	2.98	2.39
Traditional BPNN	3.36	1.52	5.74	2.42	5.49	3.71

Table 7 shows that in several risk predictions, the designed algorithm outperforms BPNN thrice and lags behind BPNN twice, but the average relative error of the designed algorithm is lower, which outperforms BPNN.

4 Conclusions

Currently, as the research on new weapons deepens, the safety risks of relevant sites have greatly increased; therefore, the safety risks of shooting test sites are explored. Quantum information theory is currently the most cutting-edge theory and scientific technology, which guides the construction of information theory in different fields and builds a brand-new theoretical framework to promote the continuous development of information technology. Here, the data obtained from the shooting test safety inspection of XXX Military Research Institute are used as the training set and test set of the experiment. By constructing a QGCNN model, the method of shooting gate safety risk assessment based on QGCNN is explored. Through simulation experiments, the effectiveness and reliability of the method are verified. The results show that the proposed model has a faster convergence speed, lower complexity of data processing, and better performance of risk prediction. Although some valuable results are achieved,

limitations are found. The risk factors analyzed cannot include some accidental factors; therefore, the designed safety management system needs improving and refining, which is also the direction of future works, thereby obtaining more comprehensive results.

References

- [1] J. Morgan, S. Pink, Researcher safety? ethnography in the interdisciplinary world of audit cultures, *Cultural Studies ↔ Critical Methodologies* 18(6)(2018) 400-409.
- [2] C. Kao, R. Furr, A unifying principle for a researcher learning safety: reduce uncertainty, *Journal of Chemical Health and Safety* 25(5)(2018) 39-40.
- [3] N. Paltrinieri, L. Comfort, G. Reniers, .Learning about risk: machine learning for risk assessment, *Safety Science* 118(2019) 475-486.
- [4] N.N. Sze, D.W.M. Chan, A.P.C. Chan, N. Yu, Implementation of safety management system in managing construction projects: benefits and obstacles, *Safety Science* 117(2019) 23-32.
- [5] K. Lee, H.-m. Kwon, s. Cho, J. Kim, I. Moon, Improvements of safety management system in Korean chemical industry after a large chemical accident, *Journal of Loss Prevention in the Process Industries* 42(2016) 6-13.
- [6] B. Guan, F. Liu, A. Haj-Mirzaian, S. Demehri, A. Samsonov, T. Neogi, A. Guermazi, R. Kijowski, Deep learning risk assessment models for predicting progression of radiographic medial joint space loss over a 48-MONTH follow-up period, *Osteoarthritis and Cartilage* 28(4)(2020) 428-437.
- [7] X. Zhang, S. Mahadevan, Ensemble machine learning models for aviation incident risk prediction, *Decision Support Systems* 116(2019) 48-63.
- [8] H. Hadeif, B. Negrou, T.G. Ayuso, M. Djebabra, M. Ramadan, Preliminary hazard identification for risk assessment on a complex system for hydrogen production, *International Journal of Hydrogen Energy* 45(20)(2020) 11855-11865.
- [9] B. Geraudie, S. Kabiche, M. Rigal, M. Malki, J.-E. Fonton, A. Jacolot, J. Schlater, Preliminary hazard analysis applied to outsourcing sterile chemotherapy preparations, *Journal of Oncology Pharmacy Practice* 25(2)(2019) 460-469.
- [10] H. Zhang, X. H, H. Mitri, Fuzzy comprehensive evaluation of virtual reality mine safety training system, *Safety Science* 120(2019) 341-351.
- [11] X. Fan, C. Li, Y. Wang, Strict intuitionistic fuzzy entropy and application in network vulnerability evaluation, *Soft Computing* 23(18)(2019) 8741-8752.
- [12] Y.-D. Cheng, J.-D. He, F.-g. Hu, Quantitative risk analysis method of information security-combining fuzzy comprehensive analysis with information entropy, *Journal of Discrete Mathematical Sciences and Cryptography* 20(1)(2017) 149-165.
- [13] A. Kierzkowski, T. Kisiel, Evaluation of a security control lane with the application of fuzzy logic., *Procedia Engineering* 187(2017) 656-663.
- [14] K.T. Schütt, M. Gastegger, A. Tkatchenko, K.-R. Müller, R.J. Maurer, Unifying machine learning and quantum chemistry with a deep neural network for molecular wavefunctions, *Nature Communications* 10(1)(2019) 146401-606.
- [15] T. Bækkegaard, L.B. Kristensen, N.J.S. Loft, C.K. Andersen, D. Petrosyan, N.T. Zinner, Realization of efficient quantum gates with a superconducting qubit-qutrit circuit, *Scientific Reports* 9(2)(2019) 467-488.

- [16] L. Gyongyowi, S. Imre, Quantum circuit design for objective function maximization in gate-model quantum computers, Quantum Information Processing 18(7)(2019) 1-16.
- [17] T. Itoko, R. Raymond, T. Imamichi, A. Matsuo, Optimization of quantum circuit mapping using gate transformation and commutation, Integration 70(2020) 43-50.
- [18] C.P. Shao, A quantum model of feed-forward neural networks with unitary learning algorithms., Quantum Information Processing 19(3)(2020) 386-408.